Giant Kerr nonlinearity and superluminal and subluminal polaritonic solitons in a Bose-Einstein condensate via superradiant scattering

Chao Hang,[1,3,*] Gregory Gabadadze,[2,3,†] and Guoxiang Huang[1,3,‡]

[1]*State Key Laboratory of Precision Spectroscopy and Department of Physics, East China Normal University, Shanghai 200062, China*

[2]*Department of Physics, New York University, New York, New York 10003, USA*

[3]*NYU-ECNU Joint Institute of Physics at NYU-Shanghai, Shanghai 200062, China*

(Received 10 June 2015; published 4 September 2015)

We propose a setup to generate giant Kerr nonlinearity and polaritonic solitons via matter-wave superradiant scattering. The system we consider is a long cigar-shaped Bose-Einstein condensate (BEC), pumped by a red-detuned laser field with a space-dependent intensity distribution in transverse directions. The pump and the scattered fields propagate along the longitudinal direction. We show that by means of the atom-photon and atom-atom interactions in the system it is possible to produce a giant nonlinear optical effect. We further show that a backward scattering of the laser field from the BEC is favorable for the formation and stable propagation of polaritonic solitons, which are collective nonlinear excitations of the BEC coupled with the scattered laser field. In the case of backward Stokes (anti-Stokes) scattering the system may support robust bright (dark) polaritonic solitons propagating with superluminal (subluminal) velocity.

DOI: 10.1103/PhysRevA.92.033805 PACS number(s): 42.65.Tg, 03.75.Kk, 32.80.Qk, 05.45.Yv

I. INTRODUCTION

Collective atomic recoil motion involving an internally generated electromagnetic field, known as matter-wave superradiance, is an intriguing process in which a group of atoms in the same electronic state recoils coherently under the excitation of a single pump laser field. Matter-wave superradiance can be regarded as an analog of Dicke's optical superradiance [1]. In addition to its fundamental role for atom optics and related research fields, the study of matter-wave superradiance also represents a promising avenue for practical applications, such as the matter-wave amplification and the fabrication of matter-wave interferometers.

In pioneering experiments on matter-wave superradiance [2–4], an elongated Bose-Einstein condensate (BEC) was used, and a continuous pump laser field was chosen to intersect along the short transverse direction of the BEC. In this setup the scattered laser field is dominated by the axial or endfire modes, while the recoiled atoms from the BEC exhibit a distinctive and highly regular pattern (side-mode distribution) due to momentum conservation. The underlying physics of this intriguing phenomenon was first explained by the scattering of pump photons off a spontaneously generated matter-wave grating that grows due to positive feedback in the presence of the pump laser [5].

Subsequently, comprehensive studies of the initial experimental observations were performed in a number of works, providing further insights into the features of the atomic momentum distribution [6–13] and the coupled dynamics of optical and matter-wave fields [14,15]. More recent theoretical works further revealed that matter-wave superradiance can be regarded as a multi-matter-optical wave-mixing process, and the propagation effect of the scattered electromagnetic waves traveling along an elongated BEC was investigated in detail [16–18].

However, up to now the majority of investigations on the propagation dynamics of matter-wave superradiance in BECs were focused on the linear regime. In this regime, polaritons are formed by a simple coupling between recoiled atoms and scattered photons; these may suffer serious spreading and attenuation during their propagation due to the existence of dispersion and nonlinearity inherent to the system. For practical applications, it is desirable to have polaritons that are robust and could propagate long distances. Thus it becomes vital to develop an approach that could take into account the dispersion and nonlinearity, and to find a setup that would yield a robust propagation of the polaritons.

In this paper, we propose a setup to create a giant Kerr nonlinearity and polaritonic solitons via matter-wave superradiant scattering in a weak recoil energy regime. The system we suggest is a long cigar-shaped BEC, pumped by a red-detuned laser field with a space-dependent intensity distribution in transverse directions. The pump and the scattered fields propagate along the longitudinal direction. We show that, due to the atom-photon and atom-atom interactions in the system, it is possible to obtain a giant nonlinear optical effect with the Kerr coefficient of the order of 10^{-5} m^2 V^{-2}; this value is at least two orders of magnitude larger than that obtained in the BEC through the mechanism of electromagnetically induced transparency (EIT) [19]. Furthermore, we show that a backward scattering of the laser field from the BEC is favorable for the formation and stable propagation of polaritonic solitons, which are collective nonlinear excitations of the BEC coupled with the scattered laser field. In addition, we demonstrate that in the case of backward Stokes (anti-Stokes) scattering the system can support robust bright (dark) polaritonic solitons propagating with superluminal (subluminal) velocity [20].

Before proceeding, we note that superluminal and subluminal optical solitons were investigated, respectively, in multilevel atomic media via EIT [21,22], and gain-assisted Raman systems [23,24]. Also, stationary polaritonic solitons

*chang@phy.ecnu.edu.cn
†gabadadze@physics.nyu.edu
‡gxhuang@phy.ecnu.edu.cn

 ©2015 American Physical Society

can be found in a BEC trapped in a soft optical lattice [25]. In addition, the creation of matter-wave vortices generated by using a Laguerre-Gaussian light beam was demonstrated to be possible [26], and a significant optical self-focusing effect in a BEC via superradiant scattering was also predicted recently [27]. Nevertheless, our work differs from Refs. [21–27], where no matter-wave superradiant scattering was considered [21–24], or no superluminal and subluminal polaritonic solitons in BECs were explored [25–27]. We expect that the giant Kerr nonlinearity and the polaritonic solitons in the BEC-based medium predicted in this work may have potential applications in nonlinear atom optics and related fields. The theoretical approach presented here can also be applied to other nonlinear dynamical problems related to matter-wave superradiance.

The remainder of the paper is organized as follows. Section II describes the theoretical model. Section III gives a linear dispersion relation, and derives the nonlinear envelope equation for polaritons in the weak recoil energy regime. Section IV studies the giant Kerr nonlinearity of the system, discusses superluminal and subluminal polaritonic solitons, and checks their stability. The last section contains the summary of the main results of the present work.

II. THE MODEL

We consider a cigar-shaped BEC coupled with a continuous-wave pump laser field $\mathbf{E}_P$ with the center wave number $\mathbf{k}_P$ and center angular frequency ω_P. Due to the interaction between the pump laser field and the atoms in the BEC, a weak pulsed scattered field $\mathbf{E}_S$ with the center wave number $\mathbf{k}_S$ and center angular frequency ω_S appears. The total electric-field vector in the system is $\mathbf{E} = \mathbf{E}_P + \mathbf{E}_S = \mathbf{e}_P \mathcal{E}_P(x,y) e^{i(\mathbf{k}_P\cdot\mathbf{r}-\omega_P t)} + \mathbf{e}_S \mathcal{E}_S(x,y,z,t) e^{i(\mathbf{k}_S\cdot\mathbf{r}-\omega_S t)}$ + c.c., where $\mathbf{e}_P$ and $\mathcal{E}_P$ ($\mathbf{e}_S$ and $\mathcal{E}_S$) are, respectively, the polarization unit vector and amplitude of the pump (scattered) field, and c.c. denotes a complex conjugate. We assume both the pump and the scattered fields have the same polarization direction, i.e., $\mathbf{e}_P = \mathbf{e}_S = \mathbf{e}_x$, and propagate along the long axis (i.e., z) direction of the BEC, i.e., $\mathbf{k}_P \cdot \mathbf{r} = k_P z$ and $\mathbf{k}_S \cdot \mathbf{r} = k_S z$. Then the electric field can be written as $\mathbf{E} = \mathbf{E}^{(+)} + \mathbf{E}^{(-)}$, with $\mathbf{E}^{(-)} = (\mathbf{E}^{(+)})^*$ and

$$\mathbf{E}^{(+)} = \mathbf{e}_x [\mathcal{E}_P(x,y) e^{i(k_P z - \omega_P t)} + \mathcal{E}_S(x,y,z,t) e^{i(k_S z - \omega_S t)}]. \quad (1)$$

The wave-vector relation and excitation scheme are shown in Fig. 1(a) [Fig. 1(b)]. The figure also depicts the wave-vector relation for the forward scattering (the backward scattering), where the scattering field propagates colinearly (anticolinearly) with the pump field. Here $\mathbf{E}_P$ and $\mathbf{k}_P$ shown by the red arrows ($\mathbf{E}_S$ and $\mathbf{k}_S$ shown by the blue arrows) are the pump field and its wave vector (the scattered field and its wave vector), respectively. The wave vector of the recoiled atoms (shown by the yellow arrow) is $\Delta\mathbf{k} = \mathbf{k}_P - \mathbf{k}_S$ for the forward scattering, or $\Delta\mathbf{k} = \mathbf{k}_P + \mathbf{k}_S$ for the backward scattering.

Figure 1(c) [Fig. 1(d)] shows the energy-level diagram for the Stokes scattering (anti-Stokes scattering), where both $\mathbf{E}_P$ and $\mathbf{E}_S$ are coupled to atomic internal states (energy levels) $|1\rangle$ and $|2\rangle$. The one-photon and two-photon detunings for the Stokes (anti-Stokes) scattering are, respectively, defined by $\Delta_1 = \omega_2 - \omega_1 - \omega_P$ and $\Delta_2 = \omega_P - \omega_S$ ($\Delta_1 = \omega_2 - \omega_1 - \omega_S$ and $\Delta_2 = \omega_S - \omega_P$), where $\hbar\omega_1$ and $\hbar\omega_2$ are, respectively, the eigenenergies of the atomic internal states $|1\rangle$ and $|2\rangle$. From this figure, we see that the light scattering process can be discussed in four different regimes, i.e., the forward Stokes scattering, the backward Stokes scattering, the forward anti-Stokes scattering, and the backward anti-Stokes scattering.

The Hamiltonian of the system is given by

$$\begin{aligned} H = & \sum_{\alpha=1}^{2} \hbar\omega_\alpha \int d\mathbf{r} \hat{\Psi}_\alpha^\dagger(\mathbf{r},t)\hat{\Psi}_\alpha(\mathbf{r},t) + \frac{\epsilon_0}{2}\int d\mathbf{r}\mathbf{E}(\mathbf{r},t)^2 \\ & + \sum_{\alpha=1}^{2} \int d\mathbf{r} \hat{\Psi}_\alpha^\dagger(\mathbf{r},t)\left[-\frac{\hbar^2}{2M}\nabla^2 + V(\mathbf{r})\right]\hat{\Psi}_\alpha(\mathbf{r},t) \\ & - \sum_{\alpha,\beta=1}^{2} \int d\mathbf{r} \hat{\Psi}_\alpha^\dagger(\mathbf{r},t)[\mathbf{p}_{\alpha\beta}\cdot\mathbf{E}(\mathbf{r},t)]\hat{\Psi}_\beta(\mathbf{r},t) \\ & + \frac{1}{2}\sum_{\alpha,\beta=1}^{2} \int d\mathbf{r}\int d\mathbf{r}' \hat{\Psi}_\alpha^\dagger(\mathbf{r},t)\hat{\Psi}_\beta^\dagger(\mathbf{r}',t)U_{\alpha\beta}(\mathbf{r}-\mathbf{r}') \\ & \times \hat{\Psi}_\beta(\mathbf{r}',t)\hat{\Psi}_\alpha(\mathbf{r},t), \end{aligned} \quad (2)$$

where $\hat{\Psi}_\alpha$ is the atomic field operator related to the state $|\alpha\rangle$ obeying the commutation relations $[\hat{\Psi}_\alpha(\mathbf{r},t),\hat{\Psi}_\beta(\mathbf{r}',t)] = [\hat{\Psi}_\alpha^\dagger(\mathbf{r},t),\hat{\Psi}_\beta^\dagger(\mathbf{r}',t)] = 0$ and $[\hat{\Psi}_\alpha(\mathbf{r},t),\hat{\Psi}_\beta^\dagger(\mathbf{r}',t)] = \delta_{\alpha\beta}\delta(\mathbf{r}-\mathbf{r}')$, M is the atomic mass, $V(\mathbf{r})$ is the trapping potential which is assumed to be the same for the two internal states, $\mathbf{p}_{\alpha\beta}$ is the electric dipole matrix element for the transition between the states $|\alpha\rangle$ and $|\beta\rangle$, $\mathbf{p}_{11} = \mathbf{p}_{22} = 0$, and $\mathbf{p}_{12} = \mathbf{p}_{21}^*$. The atom-atom interaction is described by the two-body contact potential $U_{\alpha\beta}(\mathbf{r}-\mathbf{r}') = \bar{U}_{\alpha\beta}\delta(\mathbf{r}-\mathbf{r}')$, with $\bar{U}_{\alpha\beta}$ being constants.

We assume that the one-photon detuning Δ_1 is much larger than the half Rabi frequency of the pump field Ω_P [defined below Eq. (7)]. Thus, most of the atoms in the BEC populate the state $|1\rangle$. From the Hamiltonian (2) we can get the Heisenberg equations of motion for $\hat{\Psi}_1$ and $\hat{\Psi}_2$. We use rotating-wave and adiabatic approximations to eliminate $\hat{\Psi}_2$, and obtain a closed equation for $\hat{\Psi}_1$. Then, by employing mean-field approximation, $\hat{\Psi}_1 \to \langle\hat{\Psi}_1\rangle \equiv \Psi$, one gets the modified Gross-Pitaevskii equation [12–16]:

$$\begin{aligned} i\hbar\frac{\partial}{\partial t}\Psi = & -\frac{\hbar^2}{2M}\nabla^2\Psi + V(\mathbf{r})\Psi + U_0|\Psi|^2\Psi \\ & - \frac{|\mathbf{p}_{12}\cdot\mathbf{E}^{(+)}(\mathbf{r},t)|^2}{\hbar\Delta_1}\Psi - i\hbar\Gamma(\mathbf{r},t)\Psi, \end{aligned} \quad (3)$$

where $U_0 = \bar{U}_{11} = 4\pi\hbar^2 a_s/M$ (a_s is s-wave scattering length) and $\Gamma(\mathbf{r},t) = |\mathbf{p}_{12}\cdot\mathbf{E}^{(+)}(\mathbf{r},t)|^2\Gamma_{12}/(\hbar^2\Delta_1^2)$, with Γ_{12} being the decay rate from $|2\rangle$ to $|1\rangle$.

Note that our approach is built upon a semiclassical description, which is valid when the numbers of scattered photons and recoiled atoms induced by the pump field are large enough. It is this macroscopic regime of superradiance that we are focusing on throughout our work. A fully quantized theory, on the other hand, allows us to investigate the initial stage of the superradiant process, but is not easily extended to the study of longtime propagation of the linear and nonlinear collective excitations [14–17].

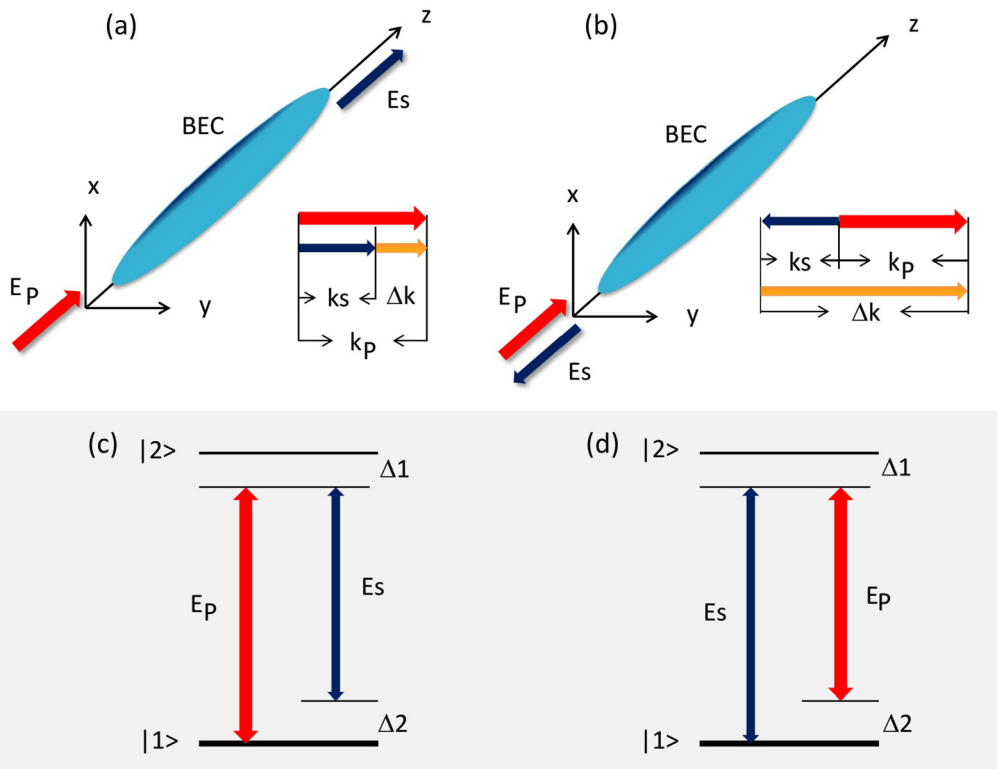

FIG. 1. (Color online) (a) [(b)] Wave-vector relation of the forward (backward) scattering from a long cigar-shaped BEC. $\mathbf{E}_P$ and $\mathbf{k}_P$ shown by red arrows ($\mathbf{E}_S$ and $\mathbf{k}_S$ shown by blue arrows) are, respectively, the pump laser field and its wave vector (scattering field and its wave vector). The wave vector of the recoiled atoms (shown by the yellow arrow) is $\Delta\mathbf{k} = \mathbf{k}_P - \mathbf{k}_S$ for the forward scattering or $\Delta\mathbf{k} = \mathbf{k}_P + \mathbf{k}_S$ for the backward scattering. (c) [(d)] Energy-level diagram for the Stokes scattering (anti-Stokes scattering). Both $\mathbf{E}_P$ and $\mathbf{E}_S$ are coupled to the atomic levels $|1\rangle$ and $|2\rangle$, with Δ_1 and Δ_2 one- and two-photon detunings, respectively. $\Delta_1 = \omega_2 - \omega_1 - \omega_P$ and $\Delta_2 = \omega_P - \omega_S$ for the Stokes scattering, or $\Delta_1 = \omega_2 - \omega_1 - \omega_S$ and $\Delta_2 = \omega_S - \omega_P$ for the anti-Stokes scattering.

The equation of motion for the electric field can be obtained from the Maxwell equation $\partial^2\mathbf{E}^{(+)}/\partial t^2 = c^2\nabla^2\mathbf{E}^{(+)} - (1/\epsilon_0)\partial^2\mathbf{P}^{(+)}/\partial t^2$, where $\mathbf{P}^{(+)} = \mathbf{p}_{12}(\mathbf{p}_{21}\cdot\mathbf{E}^{(+)})|\Psi|^2/(\hbar\Delta_1)$ is the electric polarization vector related to $\mathbf{E}^{(+)}$. When obtaining the expression for $\mathbf{P}^{(+)}$ we have employed the adiabatic approximation to eliminate $\hat{\Psi}_2$, and used the relation $\langle\hat{\Psi}_1^\dagger\hat{\Psi}_1\rangle = |\Psi|^2$. Under a slowly varying envelope approximation the Maxwell equation is reduced to

$$i\left(\frac{\partial}{\partial z} + \frac{1}{c}\frac{\partial}{\partial t}\right)\mathcal{E}_S + \frac{c}{2\omega_S}\nabla_\perp^2\mathcal{E}^{(+)} = -\frac{\omega_S}{2\epsilon_0 c}\frac{|\mathbf{p}_{12}\cdot\mathbf{e}_x|^2}{\hbar\Delta_1}\mathcal{E}^{(+)}|\Psi|^2, \quad (4)$$

where $\nabla_\perp = \partial^2/\partial x^2 + \partial^2/\partial y^2$, $\mathcal{E}^{(+)} = \mathcal{E}_P e^{i[(k_P - k_S)z - \Delta_2 t]} + \mathcal{E}_S$ for the forward Stokes scattering, $\mathcal{E}^{(+)} = \mathcal{E}_P e^{i[(k_P + k_S)z - \Delta_2 t]} + \mathcal{E}_S$ for the backward Stokes scattering, $\mathcal{E}^{(+)} = \mathcal{E}_P e^{i[(k_P - k_S)z + \Delta_2 t]} + \mathcal{E}_S$ for the forward anti-Stokes scattering, and $\mathcal{E}^{(+)} = \mathcal{E}_P e^{i[(k_P + k_S)z + \Delta_2 t]} + \mathcal{E}_S$ for the backward anti-Stokes scattering.

We consider a cigar-shaped BEC trapped in the highly anisotropic potential of the form $V(\mathbf{r}) = \frac{M}{2}[\omega_\perp^2(x^2 + y^2) + \omega_z^2 z^2]$, with $\omega_z \ll \omega_\perp$. Thus, the BEC is elongated along the z axis, but is symmetric in the x and y directions. Introducing the scaling transformations $(x', y', z') = a_\perp^{-1}(x, y, z)$, $t' = \omega_\perp t$, $\Psi = \sqrt{n_0}\psi$, and $g = \mathcal{E}_S/\mathcal{E}_P$, with $a_\perp = [\hbar/(M\omega_\perp)]^{1/2}$ being the harmonic oscillator length in the transverse (x, y) directions, and $n_0 = N/a_\perp^3$ being the atomic density, we can rewrite Eq. (3) (by dropping the primes) into the form

$$i\frac{\partial\psi}{\partial t} = -\frac{1}{2}\nabla^2\psi + \left[\frac{1}{2}(x^2 + y^2) + \frac{1}{2}\left(\frac{\omega_z^2}{\omega_\perp^2}\right)z^2\right]\psi + \frac{4\pi N a_s}{a_\perp}|\psi|^2\psi - \frac{|\mathbf{p}_{12}\cdot\mathbf{e}_x|^2}{\hbar^2}\frac{|\mathcal{E}_P|^2}{\omega_\perp\Delta_1} \times (1 + ge^{-i\Phi} + g^* e^{i\Phi} + |g|^2)\psi - i\frac{\Gamma}{\omega_\perp}\psi. \quad (5)$$

Here $\Phi = \Delta k z - \Delta\omega t$, with $\Delta k = (k_P - k_S)a_\perp$ and $\Delta\omega = \Delta_2/\omega_\perp$ for the forward Stokes scattering, $\Delta k = (k_P + k_S)a_\perp$ and $\Delta\omega = \Delta_2/\omega_\perp$ for the backward Stokes scattering, $\Delta k = (k_P - k_S)a_\perp$ and $\Delta\omega = -\Delta_2/\omega_\perp$ for the forward anti-Stokes scattering, and $\Delta k = (k_P + k_S)a_\perp$ and $\Delta\omega = -\Delta_2/\omega_\perp$ for the backward anti-Stokes scattering. Since $\omega_z^2/\omega_\perp^2 \ll 1$, the term $\frac{1}{2}(\omega_z^2/\omega_\perp^2)z^2\psi$ on the right-hand side of Eq. (5) is a small quantity for a finite condensate length, and it will be neglected in our analytical calculation below.

We assume that the BEC interacting with the pump laser field considered here can be described by a single wave function. This assumption is valid in the long-wavelength approximation for the BEC excitations, if the recoil energy of the atoms in the BEC is much smaller than the atom-field interaction energy and the atom-atom interaction energy per atom [i.e., $(\Delta k)^2 \ll |\mathbf{p}_{12}\cdot\mathbf{e}_x|^2|\mathcal{E}_P|^2/(\hbar^2\omega_\perp\Delta_1)$,

$(\Delta k)^2 \ll N a_s/a_\perp$]. In this small recoil energy regime of the superradiance, particle excitations are highly suppressed and the recoiled atoms remain in the same internal state and in the condensate. For relatively large recoil energy, however, the atoms can scatter and group into many independent side modes, and then the condensate must be described in terms of a collection of relevant side modes, while the description by a single wave function would not viable [26].

Due to the strong transverse confinement provided by the trapping potential, the condensate wave function ψ in the x and y directions behaves as a standing wave. Thus, the low-energy excitations of the BEC propagate only in the z direction. With this in mind, one can assume that $\psi = G(x,y)F(z,t)e^{-i\mu t}$ with μ being the chemical potential and $G(x,y)$ satisfying the equation [28]

$$-\frac{1}{2}\left(\frac{\partial^2}{\partial x^2}+\frac{\partial^2}{\partial y^2}\right)G+\frac{1}{2}(x^2+y^2)G=\nu G. \tag{6}$$

This is the eigenvalue equation for a two-dimensional harmonic oscillator in quantum mechanics. The ground-state solution of Eq. (6) is $G_0(x,y)=e^{-(x^2+y^2)/2}$, with the eigenvalue $\nu=1$. In addition, if the transverse distribution of the applied pump field has the Gaussian form $\mathcal{E}_P = E_0 e^{-(x^2+y^2)/(2\rho_P^2)}$, due to the strong confinement in the x and y directions provided by the trapping potential one can assume the scattered field is also of the Gaussian form, i.e., $\mathcal{E}_S = E_0 g(z,t) e^{-(x^2+y^2)/(2\rho_S^2)}$. Here ρ_P and ρ_S are, respectively, the dimensionless beam radii of the pump and scattered fields (in units $a_\perp$), and $g(z,t)$ is a dimensionless function to be determined.

With the above analysis, Eq. (5) can be simplified into the following form:

$$\begin{aligned} i\frac{\partial F}{\partial t}+\frac{1}{2}\frac{\partial^2 F}{\partial z^2}+(\mu-1)F-c_1|F|^2F \\ +c_2(1+ge^{-i\Phi}+g^*e^{i\Phi}+|g|^2)F+i\gamma F=0, \end{aligned} \tag{7}$$

with $c_1 = 2\pi N a_s/a_\perp$, $c_2 = |\Omega_P|^2\rho^2/[(\omega_\perp\Delta_1)(1+\rho^2)]$, and $\gamma = \Gamma/\omega_\perp$. Here we have defined the half Rabi frequency of the pump field $\Omega_P = (\mathbf{p}_{12}\cdot\mathbf{e}_x)E_0/\hbar$ and assumed that $\rho_P = \rho_S \equiv \rho$ [29]. Note that for obtaining Eq. (7) we have used Eq. (6) with $G(x,y) = G_0(x,y)$ and multiplied Eq. (5) by $G_0^*(x,y)$ and then integrated it once with respect to x and y.

Equation (4) can also be converted into the dimensionless form

$$i\left(\frac{\partial}{\partial z}+\frac{1}{v}\frac{\partial}{\partial t}\right)g-d_1(e^{i\Phi}+g)+d_2(e^{i\Phi}+g)|F|^2=0, \tag{8}$$

with $v = c/(a_\perp\omega_\perp)$, $d_1 = c/(2\omega_S a_\perp\rho^2)$, and $d_2 = N\omega_S|\mathbf{p}_{12}\cdot\mathbf{e}_x|^2/[(2\epsilon_0 c\hbar a_\perp^2\Delta_1)(1+\rho^2)]$. For obtaining the above equation, we have multiplied Eq. (4) by $e^{-(x^2+y^2)/(2\rho^2)}$ and then integrated it once with respect to x and y. Note that Eqs. (7) and (8) are quasi-one-dimensional and hence convenient for a detailed theoretical analysis.

The model described above can be realized by a practical physical system consisting of a condensed ^{87}Rb atomic gas with the atomic internal states assigned as $|1\rangle = |5^2S_{1/2}\rangle$ and $|2\rangle = |5^2P_{1/2}\rangle$. The other system parameters are given as $a_s = 94.8a_0$, $|\mathbf{p}_{12}| = 2.54\times10^{-27}$ C cm, $\Gamma_{12}/(2\pi) = 5.7$ MHz, and n_0 (atomic density)$= 4.0\times10^{19}\,\mathrm{m}^{-3}$. We further fix $\omega_\perp/(2\pi) = 100$ Hz, resulting in $a_\perp \approx 1.1\,\mu$m, and $\omega_z/(2\pi) = 0.1$ Hz. All calculations given below will be based on these parameters.

III. ASYMPTOTIC EXPANSION AND NONLINEAR ENVELOPE EQUATIONS

Now we turn to solve Eqs. (7) and (8). To understand the properties of excitation of the system, one should first know its ground state (i.e., the homogeneous stationary background of the condensate along the z direction). The latter can be obtained from Eqs. (7) and (8) by neglecting the derivative terms and setting $f = f_0$, $g = 0$; this yields

$$(\mu-1)f_0-c_1f_0^3+c_2f_0=0, \tag{9a}$$

$$-d_1+d_2f_0^2=0. \tag{9b}$$

Note that we have also set $\gamma = 0$ for the ground state since it is a small quantity and plays no significant role in the stationary background of the BEC (nonzero γ will be considered in the higher-order dynamics). From Eqs. (9a) and (9b), one obtains the solution $f_0 = \sqrt{(\mu-1+c_2)/c_1} = \sqrt{d_1/d_2}$, which leads to the chemical potential $\mu = 1-c_2+c_1d_1/d_2$. The length of the BEC, denoted by L, can be determined by the normalization condition $\int_0^L dz f_0^2 = 1$ (derived from $\int d\mathbf{r}|\Psi|^2 = N$), resulting in $L = d_2/d_1$.

Equation (9b) requires $f_0^2 = d_1/d_2$, which leads to the following conclusions.

(i) Since d_1 is positive, d_2 should also be positive, which means that $\Delta_1 > 0$. Thus the stationary background of the BEC can exist only when the pump field is red-detuned. This conclusion agrees with the experimental result reported in Ref. [11], where a blue-detuned pump laser was used and an efficient suppression of matter-wave superradiance was observed.

(ii) If the pump field is homogeneous in the transverse directions, i.e., $\rho\to+\infty$ ($d_1\to0$), the second equation will reduce to $d_2f_0^2=0$, i.e., $f_0=0$; in this case all atoms would be recoiled into the states of external motion and no stationary background of the condensate would exist. Thus the transverse spatial distribution of the pump field [i.e., $\mathcal{E}_P = \mathcal{E}_P(x,y)$] is necessary for the existence of the stationary background of the BEC, which guarantees the viability of the assumption of the weak recoil regime mentioned above.

We use the standard perturbation theory [30] to study the linear and nonlinear excitations of the BEC and the scattered field in the system. To this end, we perform the asymptotic expansions, $F = f_0+\sum_{n=1}^{\infty}\epsilon^n f^{(n)}$ and $g = \sum_{n=1}^{\infty}\epsilon^n g^{(n)}$, with ϵ being a small parameter, proportional to the typical amplitude of the scattered field. All quantities on the right-hand side of the expansions are assumed to be functions of the multiscale variables $t_j = \epsilon^j t$ $(j=0,1,2)$ and $z_j = \epsilon^j z$ $(j=0,1)$. In addition, γ is assumed to be of the order of ϵ. Then,

Eqs. (7) and (8) become

$$i\left(\frac{\partial}{\partial t_0}+\gamma\right)f^{(j)}+\frac{1}{2}\frac{\partial^2 f^{(j)}}{\partial z_0^2}-c_1 f_0^2(f^{(j)}+f^{(j)*}) +c_2 f_0(g^{(j)}e^{-i\phi}+g^{(j)*}e^{i\phi})=M^{(j)}, \tag{10a}$$

$$i\left(\frac{\partial}{\partial z_0}+\frac{1}{v}\frac{\partial}{\partial t_0}\right)g^{(j)}+d_2 e^{i\phi}f_0(f^{(j)}+f^{(j)*})=N^{(j)} \tag{10b}$$

($j=1,2,3,\ldots$) with $\phi=\Delta k z_0-\Delta\omega t_0$. The explicit expressions for $M^{(j)}$ and $N^{(j)}$ ($j=1,2,3$) are given in the Appendix.

Following the standard approach [31,32] for seeking the collective Bogoliubov excitation (i.e., density fluctuation) in the BEC, and for the scattered light field induced by the pump field, we assume $f^{(j)}=f_+^{(j)}e^{i\varphi}+f_-^{(j)*}e^{-i\varphi}$ with $\varphi=qz_0-\omega_q t_0$. Here q and ω_q are, respectively, the dimensionless atomic recoil momentum and the corresponding atomic recoil energy induced by the light scattering process. Then, Eqs. (10) turn into the following equations for $f_+^{(j)}$, $f_-^{(j)}$, and $g^{(j)}$:

$$i\left(\frac{\partial}{\partial t_0}+q\frac{\partial}{\partial z_0}+\gamma\right)f_+^{(j)}+\left(\omega_q-\frac{q^2}{2}-c_1 f_0^2\right)f_+^{(j)} +\frac{1}{2}\frac{\partial^2 f_+^{(j)}}{\partial z_0^2}-c_1 f_0^2 f_-^{(j)}+c_2 f_0 g^{(j)*}e^{i\xi}=M^{(j)}e^{-i\varphi}, \tag{11a}$$

$$i\left(\frac{\partial}{\partial t_0}-q\frac{\partial}{\partial z_0}+\gamma\right)f_-^{(j)}+\left(\omega_q+\frac{q^2}{2}+c_1 f_0^2\right)f_-^{(j)} -\frac{1}{2}\frac{\partial^2 f_-^{(j)}}{\partial z_0^2}+c_1 f_0^2 f_+^{(j)}-c_2 f_0 g^{(j)*}e^{i\xi}=-M^{(j)*}e^{-i\varphi}, \tag{11b}$$

$$i\left(\frac{\partial}{\partial z_0}+\frac{1}{v}\frac{\partial}{\partial t_0}\right)g^{(j)}+d_2 f_0(f_+^{(j)*}+f_-^{(j)*})e^{i\xi}=N^{(j)}, \tag{11c}$$

with $\xi=\phi-\varphi=(\Delta k-q)z_0-(\Delta\omega-\omega_q)t_0$. Obviously, phase matching is achieved if $\xi\approx 0$, or

$$q=\Delta k,\quad \omega_q=\Delta\omega. \tag{12}$$

That is to say, the Bogoliubov excitation of the BEC provides the phase $\varphi=qz_0-\omega_q t_0$ that may compensate the phase mismatch between the laser field and the atomic transition. Recalling that $\Delta k=(k_P\mp k_S)a_\perp$ ("+" for the backward scattering; "−" for the forward scattering) and $\Delta\omega=\pm\Delta_2/\omega_\perp$ ("+" for the Stokes scattering; "−" for the anti-Stokes scattering), we expect various efficient light scatterings can occur in the system under the phase-matching condition (12).

Equations (11) can be solved order by order in a systematic way. In the first-order ($j=1$) approximation, by assuming that the solution of Eqs. (11) ($f_+^{(1)}$, $f_-^{(1)}$, and $g^{(1)*}$) is proportional to $e^{i(kz_0-\omega t_0)}$, we obtain

$$(\omega+\omega_q+i\gamma)^2-(k+q)^2 \times\left[\frac{(k+q)^2}{4}+c_1 f_0^2+\frac{c_2 d_2 f_0^2}{k-\omega/v}\right]=0. \tag{13}$$

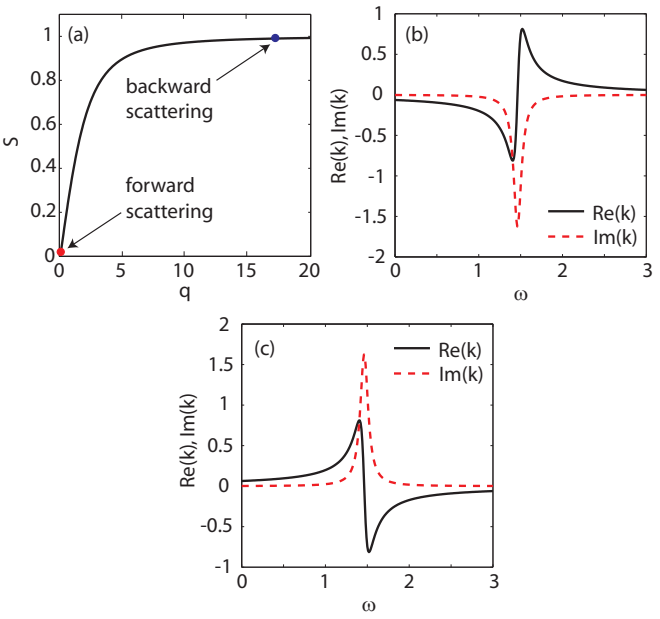

FIG. 2. (Color online) (a) BEC structure factor $S(q)$ as a function of q. The red (blue) solid circle corresponds to the forward (backward) scattering at $(q,S(q))\approx(0,0)$ $[(q,S(q))\approx(17,0.99)]$. (b) Re($k$) (black solid line) and Im(k) (red dashed line) as functions of ω for the backward Stokes scattering ($q\approx 17$, $\omega_q\approx\omega_B$). (c) Re(k) (black solid line) and Im(k) (red dashed line) as functions of ω for the backward anti-Stokes scattering ($q\approx 17$, $\omega_q\approx-\omega_B$).

Since k can be treated as a small deviation from q ($\approx\Delta k$), we can use the approximation $k+q\approx q$. As a result, we get from Eq. (13)

$$k(\omega)=\frac{\omega}{v}+c_2 d_2 f_0^2 S(q)\left(\frac{1}{\omega+\omega_q+i\gamma-\omega_B} -\frac{1}{\omega+\omega_q+i\gamma+\omega_B}\right), \tag{14}$$

where $S(q)=q^2/(2\omega_B)$ is the BEC structure factor, and $\omega_B=q\sqrt{q^2/4+c_1 f_0^2}$ is the angular frequency of the Bogoliubov excitation in the BEC. Equation (14) gives the linear dispersion relation for a polariton, a quasiparticle that is a superposition of the scattered light and matter wave of the system.

From the expression (14), we see that the BEC structure factor $S(q)$ significantly affects the dispersive property of the system. Specifically, the system is weakly (strongly) dispersive when $S(q)$ is small (large). On the other hand, $S(q)\approx q/(2\sqrt{c_1}f_0)$ when $q^2/4\ll c_1 f_0^2$, and $S(q)\approx 1$ when $q^2/4\gg c_1 f_0^2$. Consequently, if the scattering field propagates colinearly with the pump field (forward scattering), one has $q\approx\Delta k\approx(k_P-k_S)a_\perp$, resulting in a small $S(q)$, and hence the system is weakly dispersive. However, if the scattering field propagates anticolinearly with the pumping field (backward scattering), one has $q\approx\Delta k\approx(k_P+k_S)a_\perp$, resulting in the large $S(q)$ and strongly dispersive system.

In Fig. 2(a) we show $S(q)$ as a function of q. To be specific, we take $N=500$, $\Delta_1=1.0$ GHz, $\Omega_P=1.0$ MHz, $\rho=1.0$, and $\omega=0$. With these parameters, we have $\mu\approx 0.87$, $f_0\approx 0.32$, $\gamma\approx 0.06$, and $L\approx 10$. It is clear that $S(q)$

increases rapidly as long as q is small ($q \lesssim 5$), and saturates by approaching 1.0 when q becomes large ($q \gtrsim 10$). For the forward scattering $q \approx 0$ (the red solid circle) one has $S(q) \approx 0$, and for the backward scattering $q \approx 17$ (the blue solid circle) one has $S(q) \approx 0.99$.

Note that there are two terms in parentheses in the linear dispersion relation (14), which correspond, respectively, to the Stokes and anti-Stokes scattering; the two terms have very different contributions to the nonlinear evolution of the polariton in the system, hence in what follows we discuss them separately.

A. Stokes scattering

In this case, $\omega_P > \omega_S$. One has $\omega_q \approx \Delta\omega = \Delta_2/\omega_\perp > 0$ and hence $\omega_q - \omega_B \ll \omega_q + \omega_B$. Thus the second term in parentheses in Eq. (14) is much smaller than the first term and can be neglected. As a result, we get

$$k(\omega) \approx \frac{\omega}{v} + c_2 d_2 f_0^2 S(q) \frac{1}{\omega + \omega_q + i\gamma - \omega_B}. \tag{15}$$

From this result it is easy to show that the imaginary part of k, denoted by $\mathrm{Im}(k)$, is negative around $\omega = 0$; this means that the scattering field has a gain. The solution in this order is given by $f_+^{(1)} = Ae^{i(kz_0 - \omega t_0)}$, $f_-^{(1)} = aAe^{i(kz_0 - \omega t_0)}$, and $g^{(1)*} = bAe^{i(kz_0 - \omega t_0)}e^{-i\xi}$, with

$$a = \frac{X}{c_1 f_0^2 + c_2 d_2 f_0^2/(k - \omega/v)}, \quad b = -\frac{d_2 f_0 (1 + a)}{k - \omega/v},$$

where $X = \omega + \omega_q + i\gamma - q^2/2 - c_1 f_0^2 - c_2 d_2 f_0^2/(k - \omega/v)$, and A is a yet to be determined envelope function.

Shown in Fig. 2(b) are $\mathrm{Re}(k)$ (black solid line) and $\mathrm{Im}(k)$ (red dashed line) as functions of ω for the backward Stokes scattering ($q \approx 17$, $\omega_q \approx \omega_B$), which describe the dispersion [$\mathrm{Re}(k)$] and gain [in the region for $\mathrm{Im}(k) < 0$] or loss [in the region for $\mathrm{Im}(k) > 0$], respectively. We see that a steep dispersion with positive slope and a maximum gain can be observed near $\omega = 0$.

At the next order ($j = 2$), the solvability condition of Eq. (11) requires

$$i\left(\frac{\partial A}{\partial z_1} + \frac{1}{V_g}\frac{\partial A}{\partial t_1}\right) = 0, \tag{16}$$

where V_g is the group velocity of the envelope A, given by

$$V_g^{-1} = \frac{\partial k(\omega)}{\partial \omega} = \frac{1}{v} - c_2 d_2 f_0^2 S(q) \frac{(\delta - i\gamma)^2}{(\delta^2 + \gamma^2)^2} \times \left[1 - \frac{2(\delta - i\gamma)}{(\delta^2 + \gamma^2)}\omega\right], \tag{17}$$

with $\delta = \omega_q - \omega_B$. Since $1/v$ is very small [$v = c/(a_\perp \omega_\perp) \approx 4.4 \times 10^{11}$ for the adopted values of the parameters], $\mathrm{Re}(V_g)$ is negative around $\omega = 0$, corresponding to a superluminal propagation of the polariton.

The evolution of the envelope function A in the nonlinear regime can be obtained by the solvability condition in the third-order approximation ($j = 3$) of Eq. (11), with the result given by

$$i\frac{\partial A}{\partial z_2} + \frac{D}{2}\frac{\partial^2 A}{\partial t_1^2} + W|A|^2 A e^{-2\tilde{\alpha} z_2} = 0, \tag{18}$$

with

$$D = \frac{\partial^2 k(\omega)}{\partial \omega^2} = 2c_2 d_2 f_0^2 S(q) \frac{(\delta - i\gamma)^3}{(\delta^2 + \gamma^2)^3}, \tag{19a}$$

$$W = -\frac{1}{Z}\Big\{Y[c_1(1 + 2a^2) - c_2 b^2] - \left(c_1 f_0^2 + \frac{c_2 d_2 f_0^2}{k - \omega/v}\right)[c_1(2 + a^2) - c_2 b^2]a + \left(\omega + \omega_q + i\gamma + \frac{q^2}{2}\right)\frac{c_2 d_2 f_0}{k - \omega/v}(1 + a^2)b\Big\}, \tag{19b}$$

where $Y = \omega + \omega_q + i\gamma + q^2/2 + c_1 f_0^2 + c_2 d_2 f_0^2/(k - \omega/v)$, $Z = (\omega + \omega_q + i\gamma + q^2/2)[q + c_2 f_0 b/(k - \omega/v)] + q[c_1 f_0^2 + c_2 d_2 f_0^2/(k - \omega/v)](1 - a)$, and $\tilde{\alpha} = \epsilon^{-2}\alpha = \epsilon^{-2}\mathrm{Im}(k)$. The real parts of the coefficients D and W [i.e., $\mathrm{Re}(D)$ and $\mathrm{Re}(W)$] characterize the group-velocity dispersion and Kerr nonlinearity of the system, respectively.

B. Anti-Stokes scattering

In this case, $\omega_P < \omega_S$. One has $\omega_q \approx \Delta\omega = -\Delta_2/\omega_\perp < 0$ and hence $\omega_q + \omega_B \ll \omega_q - \omega_B$. Thus the first term in the parentheses of Eq. (14) is much smaller than the second one and can be neglected. As a result, Eq. (14) reduces to

$$k(\omega) \approx \frac{\omega}{v} - c_2 d_2 f_0^2 S(q) \frac{1}{\omega + \omega_q + i\gamma + \omega_B}. \tag{20}$$

It is straightforward to show that the imaginary part, $\mathrm{Im}(k)$, is positive around $\omega = 0$; therefore, the scattering field is being attenuated during its propagation. Figure 2(c) shows $\mathrm{Re}(k)$ (black solid line) and $\mathrm{Im}(k)$ (red dashed line) as functions of ω for the backward anti-Stokes scattering ($q \approx 17$, $\omega_q \approx -\omega_B$), describing the dispersion [$\mathrm{Re}(k)$] and gain [in the region for $\mathrm{Im}(k) < 0$] or loss [in the region for $\mathrm{Im}(k) > 0$], respectively.

In the second-order approximation ($j = 2$), the solvability condition of Eq. (11) results in Eq. (16) again, but now the group velocity is given by

$$V_g^{-1} = \frac{1}{v} + c_2 d_2 f_0^2 S(q) \frac{(\delta - i\gamma)^2}{(\delta^2 + \gamma^2)^2}\left[1 - \frac{2(\delta - i\gamma)}{(\delta^2 + \gamma^2)}\omega\right]. \tag{21}$$

In contrast with the Stokes scattering, $\mathrm{Re}(V_g)$ for the anti-Stokes scattering is positive around $\omega = 0$, which means that the polariton in this case has a subluminal propagation velocity.

In the third-order approximation ($j = 3$), one can also derive the evolution equation for the envelope function A from Eq. (11), which has the same form as Eq. (18) but the coefficient of the group-velocity dispersion is replaced by

$$D = -2c_2 d_2 f_0^2 S(q) \frac{(\delta - i\gamma)^3}{(\delta^2 + \gamma^2)^3}. \tag{22}$$

The latter has a different sign as compared to the case of the Stokes scattering.

IV. GIANT KERR NONLINEARITY AND POLARITONIC SOLITONS

The possibility to observe nonlinear optical effects is one of the most fascinating aspects of ultracold quantum gases. Since the BEC in our setup is illuminated by a laser, the nonlinear optical properties are affected not only by the atom-atom interaction but also by the atom-photon coupling. Thus, one might expect to produce an enhanced nonlinear optical effect in the present system, that is not available in conventional quantum gases.

For not too high light intensity, the nonlinear optical effect can be estimated by using the relation $n = n_0 + n_2 I$, where n is the total refractive index, n_0 is the linear refractive index, n_2 is the Kerr coefficient, and $I = |\mathbf{E}|^2/2$ is the light intensity. In the system at hand, it is straightforward to show that n_2 is determined by the relation $n_2 = -[c/(\omega_S E_0^2 b^2 a_\perp)]W$, with W given in Eq. (19b). Figure 3(a) shows the real (black solid line) and imaginary (red dashed line) parts of n_2, i.e., $\mathrm{Re}(n_2)$ and $\mathrm{Im}(n_2)$, as functions of δ for the backward scattering ($q \approx 17$). The values of the physical parameters used in this figure are the same as those in Fig. 2 with $\omega = 0$. One can see that the minimal value of $\mathrm{Re}(n_2)$ is about $1.9 \times 10^{-8}\,\mathrm{m^2\,V^{-2}}$ at $\delta \approx \pm 1.3$. In Fig. 3(b) we show the same functions for the forward scattering ($q \approx 0$). The minimal value of $\mathrm{Re}(n_2)$ is about $1.6 \times 10^{-5}\,\mathrm{m^2\,V^{-2}}$ at $\delta = 0$. Because a weak electric field is implied by the assumed small recoil energy regime of the superradiance, n_0 is still much larger than $n_2 I$.

From the above result, one can deduce that the Kerr coefficient n_2 in the present system is at least 15 orders of magnitude larger than that measured in usual nonlinear optical materials, such as optical fibers [33]. It is also at least two orders of magnitude larger than that obtained in a BEC-based EIT system reported by Hau *et al.* [19], where $n_2 \approx 1.05 \times 10^{-7}\,\mathrm{m^2\,V^{-2}}$ was shown to be possible. The physical reasons for the giant Kerr nonlinearity obtained here are mainly due to the high atomic density and the strong photon-atom and atom-atom interaction in the BEC.

Now we turn to the formation and propagation of superluminal and subluminal polaritonic solitons in the system. In contrast with the forward scattering, the backward scattering can provide a larger dispersion which is required for balancing the Kerr nonlinearity, and hence it is more favorable for the formation and propagation of polaritonic solitons. Combining

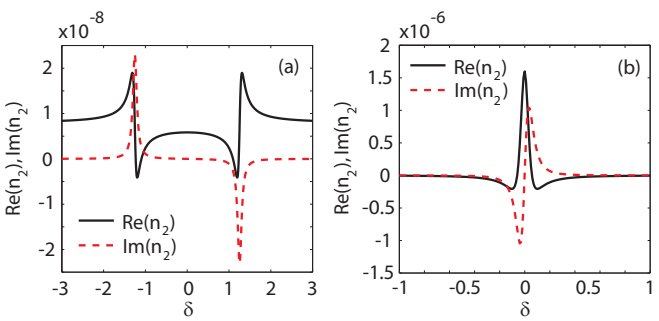

FIG. 3. (Color online) $\mathrm{Re}(n_2)$ (black solid line) and $\mathrm{Im}(n_2)$ (red dashed line) as functions of δ for the backward scattering ($q \approx 17$) (a) and the forward scattering ($q \approx 0$) (b). In both panels, $\omega = 0$.

Eqs. (16) and (18) we obtain

$$i\frac{\partial U}{\partial z} + \frac{\mathrm{Re}(D)}{2}\frac{\partial^2 U}{\partial \tau^2} + \mathrm{Re}(W)|U|^2 U = -i\alpha U, \tag{23}$$

where $U = \epsilon A e^{-\alpha z}$ and $\tau = t - z/\mathrm{Re}(V_g)$.

Equation (23) has the form of the nonlinear Schrödinger equation, with the term on the right-hand side describing the effect of the gain or loss. While deriving Eq. (23) we have assumed that the imaginary parts of V_g, D, and W, are much smaller than their corresponding real parts, and hence they were neglected. This assumption is justified under the conditions $\gamma \ll 1$ (which can be achieved by satisfying $|\Omega_p|^2/\Delta^2 \ll 1$) and $\delta \gg \gamma$. In addition, due to $|\alpha| \ll 1$ the gain or loss term on the right-hand side of Eq. (23) can be neglected in the first order. Thus, one can have a stable bright soliton solution $U = \sqrt{2/|\mathrm{Re}(W)|}\,\mathrm{sech}[\sqrt{2/|\mathrm{Re}(D)|}\,\tau]e^{i\sigma z}$ if the coefficients fulfill the condition $\mathrm{Re}(DW) > 0$ or, alternatively, a stable dark soliton solution $U = \sqrt{2/|\mathrm{Re}(W)|}\tanh[\sqrt{2/|\mathrm{Re}(D)|}\,\tau]e^{i\sigma z}$ if the coefficients satisfy $\mathrm{Re}(DW) < 0$. Here $\sigma = 1$ ($\sigma = -1$) if $\mathrm{Re}(D) > 0$ [$\mathrm{Re}(D) < 0$]. Since W can be turned to be either positive or negative by changing the values of the parameters, the system can support bright or dark solitons.

By returning to the original (i.e., dimensional) variables, we can write the following expression for the wave function:

$$\Psi = \frac{N^{1/2}}{a_\perp^{3/2}}[f_0 + U e^{i(q+k)z/a_\perp - i(\omega_q+\omega)\omega_\perp t} + a^* U^* e^{-i(q+k)z/a_\perp + i(\omega_q+\omega)\omega_\perp t}]e^{-i\mu\omega_\perp t}e^{-(x^2+y^2)/(2a_\perp^2)}, \tag{24}$$

and the scattered field $\mathbf{E}_S = \mathbf{e}_x \mathcal{E}_S e^{ik_S z - i\omega_S t} + \mathrm{c.c.}$, with

$$\mathcal{E}_S = E_0 b^* U^* e^{-ikz/a_\perp + i\omega\omega_\perp t} e^{-(x^2+y^2)/(2\rho_S^2 a_\perp^2)}. \tag{25}$$

From the solution (24) we see that the matter waves (the collective waves of recoiled atoms) consist of two parts, the left- and right-moving parts along the z axis. For the backward scattering, one has $|a| \ll 1$ and $|b| \sim 1$ [e.g., $a \approx (1.5 - i2.0) \times 10^{-4}$ and $b \approx 3.0 - i0.1$ with $\delta = -1.5$]. Thus almost all recoiled atoms are moving to the right due to the presence of the pump field, while the scattered field is propagating to the left [see Fig. 1(b)].

Let us now choose a set of parameters to demonstrate that the system we proposed indeed supports different types of polaritonic solitons. Since we are interested in the backward scattering (which has a stronger dispersion that favors the formation of solitons), we fix $q \approx 17$ and hence $S(q) \approx 1$. For the Stokes scattering, using the parameters given in Fig. 2 and $\delta = -1.5$, we obtain that $k \approx -(6.18 + i0.23) \times 10^{-2}$, $v_g \approx -24.31 + i1.86$, $D \approx -(5.43 + i0.62) \times 10^{-2}$, and $W \approx -1.85 - i0.17$. One can see that the imaginary parts of these quantities are indeed much smaller than their corresponding real parts. Furthermore, Eq. (23) supports a bright polaritonic soliton solution $U \approx 1.04\,\mathrm{sech}[6.07(t + 0.04z)]e^{-iz}$, propagating with a superluminal group velocity:

$$V_g \approx -1.59 \times 10^{-2}\,\mathrm{m\,s^{-1}}. \tag{26}$$

For the anti-Stokes scattering, we obtain that $k \approx (6.18 + i0.23) \times 10^{-2}$, $v_g \approx 24.31 - i1.86$, $D \approx (5.43 + i0.62) \times 10^{-2}$, and $W \approx -1.04 + i0.28$. In this case Eq. (23) supports

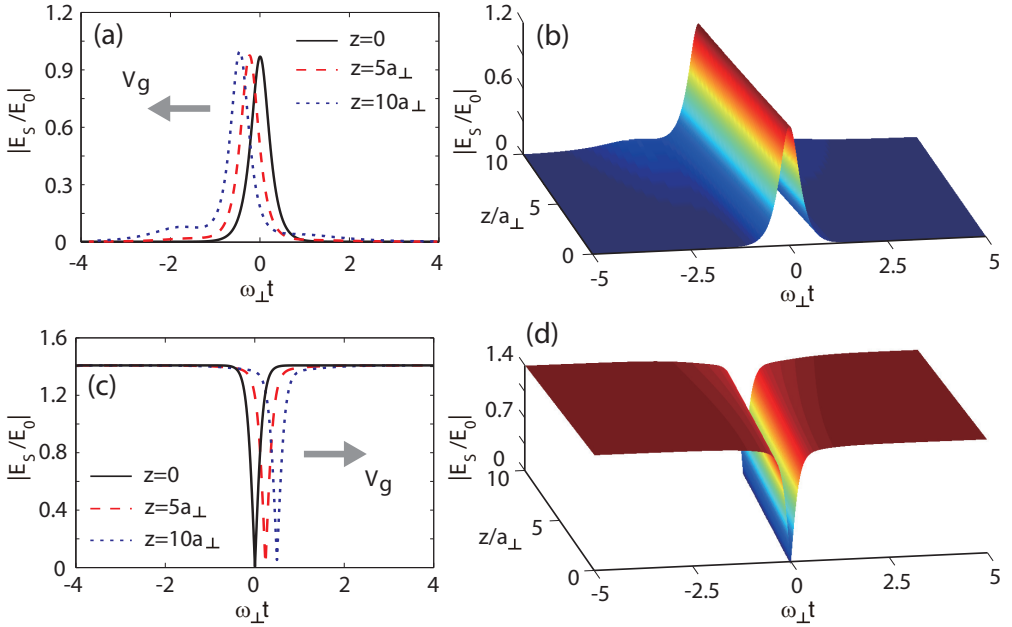

FIG. 4. (Color online) (a) Bright soliton profile of the scattering field, $|E_S/E_0|$, for the backward Stokes scattering as a function of $\omega_\perp t$. The black solid line, red dashed line, and blue dotted line are for the propagating distance $z = 0, 5\,a_\perp$, and $10\,a_\perp$, respectively. The propagating velocity of the soliton is negative (shown by the gray arrow), corresponding to a superluminal propagation. (b) Three-dimensional plot of the bright soliton. (c) Dark soliton profile of the scattering field for the backward anti-Stokes scattering. The black solid line, red dashed line, and blue dotted line are for the propagating distance $z = 0$, $5\,a_\perp$, and $10\,a_\perp$, respectively. The group velocity of the soliton is positive (shown by the gray arrow), corresponding to a subluminal propagation. (d) Three-dimensional plot of the dark soliton.

the dark polaritonic soliton solution, $U = 1.39\tanh[6.07(t - 0.04z)]e^{-iz}$, propagating with a subluminal velocity:

$$V_g \approx 1.59 \times 10^{-2}\ \mathrm{m\,s^{-1}}. \tag{27}$$

In order to confirm the analytical results obtained above, we have carried out numerical simulations on the propagation of polaritonic solitons based on Eqs. (7) and (8), with the results shown in Fig. 4. The maximum propagation distance is $z = 10a_\perp \approx 22\,\mu$m, corresponding to the length of the BEC. In Fig. 4(a) we show the bright soliton profile of the scattered field, $|E_S/E_0|$, for the backward Stokes scattering as a function of $\omega_\perp t$. The black solid line, red dashed line, and blue dotted line are for the propagation distance $z = 0$, $5\,a_\perp$, and $10\,a_\perp$, respectively. The propagation velocity of the soliton in the Stokes scattering is negative, indicated by the gray arrow, which means a superluminal propagation. Shown in Fig. 4(b) is the three-dimensional plot of the bright soliton given in Fig. 4(a). In Fig. 4(c) we show the dark soliton profile of the scattering field for the backward anti-Stokes scattering, with the black solid line, red dashed line, and blue dotted line being for $z = 0$, $5\,a_\perp$, and $10\,a_\perp$, respectively. The group velocity of the dark soliton is positive (shown by the gray arrow), corresponding to a subluminal propagation. Figure 4(d) is the three-dimensional plot of the dark soliton given in Fig. 4(c). We see that both the bright and the dark polaritonic solitons are fairly stable during their propagation in the BEC.

V. DISCUSSIONS AND SUMMARY

In this paper we have proposed a scheme for generating giant Kerr nonlinearity and polaritonic solitons via matter-wave superradiant scattering. The system we suggest is a long cigar-shaped BEC, pumped by a red-detuned laser field with a space-dependent intensity distribution in transverse directions. The pump and the scattered fields propagate along the longitudinal direction. We have shown that due to the atom-photon and atom-atom interactions in the system it is possible to produce a giant nonlinear optical effect. Furthermore, we have shown that a backward scattering of the laser field from the BEC is favorable for the formation and stable propagation of polaritonic solitons. In addition, we have demonstrated that in the case of backward Stokes (anti-Stokes) scattering the system can support robust bright (dark) polaritonic solitons propagating with superluminal (subluminal) velocity.

We expect that the giant Kerr nonlinearity and the polaritonic solitons in the superradiant scattering of BEC predicted in this work may have potential applications in nonlinear atom optics and related fields. The theoretical approach presented here can be applied to other nonlinear problems (e.g., four-wave mixing and generation and propagation of two coupled polaritons) related to matter-wave superradiance.

ACKNOWLEDGMENTS

The authors would like to thank Dr. Haibin Wu for fruitful discussions. The work of C.H. and G.H. was supported by National Natural Science Foundation of China under Grants No. 11475063, No. 11174080, and No. 11474099. G.G. would like to thank the Department of Physics of East China Normal University, for warm hospitality.

APPENDIX: EXPRESSIONS OF $M^{(j)}$ and $N^{(j)}$ ($j = 1, 2, 3$)

In the first order ($j = 1$), $M^{(1)} = N^{(1)} = 0$. In the second order ($j = 2$),

$$M^{(2)} = -i\frac{\partial f^{(1)}}{\partial t_1} - \frac{\partial^2 f^{(1)}}{\partial z_0 \partial z_1} + c_1 f_0(2|f^{(1)}|^2 + f^{(1)\,2}) - c_2 f_0 |g^{(1)}|^2 - c_2 f^{(1)}(g^{(1)*}e^{i\Phi} + g^{(1)}e^{-i\Phi}), \tag{A1}$$

$$N^{(2)} = -i\frac{\partial g^{(1)}}{\partial z_1} - d_2|f^{(1)}|^2 e^{i\Phi} - d_2 f_0(f^{(1)*} + f^{(1)})g^{(1)}. \tag{A2}$$

In the third order ($l = 3$),

$$M^{(3)} = -i\frac{\partial f^{(2)}}{\partial t_1} - i\frac{\partial f^{(1)}}{\partial t_2} - \frac{\partial^2 f^{(2)}}{\partial z_0 \partial z_1} - \frac{1}{2}\frac{\partial^2 f^{(1)}}{\partial z_1^2} - \frac{\partial^2 f^{(1)}}{\partial z_0 \partial z_2} + c_1[2f_0(f^{(1)}f^{(2)*} + f^{(1)}f^{(2)} + f^{(1)*}f^{(2)}) + |f^{(1)}|^2 f^{(1)}]$$
$$- c_2(f_0 g^{(1)}g^{(2)*} + f_0 g^{(1)*}g^{(2)} + f^{(1)}|g^{(1)}|^2) - c_2(f^{(1)}g^{(2)*} + f^{(2)}g^{(1)*})e^{i\Phi} - c_2(f^{(1)}g^{(2)} + f^{(2)}g^{(1)})e^{-i\Phi}, \tag{A3}$$

$$N^{(3)} = -i\frac{\partial g^{(2)}}{\partial z_1} - i\frac{\partial g^{(1)}}{\partial z_2} - d_2(f^{(1)}f^{(2)*} + f^{(1)*}f^{(2)})e^{i\Phi} - d_2[f_0(f^{(1)*} + f^{(1)})g^{(2)} + f_0(f^{(2)*} + f^{(2)})g^{(1)} + |f^{(1)}|^2 g^{(1)}]. \tag{A4}$$

[1] R. H. Dicke, Coherence in spontaneous radiation processes, Phys. Rev. **93**, 99 (1954).

[2] S. Inouye, A. P. Chikkatur, D. M. Stamper-Kurn, J. Stenger, D. E. Pritchard, and W. Ketterle, Superradiant Rayleigh scattering from a Bose-Einstein condensate, Science **285**, 571 (1999).

[3] D. Schneble, Y. Torii, M. Boyd, E. W. Streed, D. E. Pritchard, and W. Ketterle, The onset of matter-wave amplification in a superradiant Bose-Einstein condensate, Science **300**, 475 (2003).

[4] S. Inouye, R. F. Low, S. Gupta, T. Pfau, A. Gorlitz, T. L. Gustavson, D. E. Pritchard, and W. Ketterle, Amplification of Light and Atoms in a Bose-Einstein Condensate, Phys. Rev. Lett. **85**, 4225 (2000).

[5] M. G. Moore and P. Meystre, Theory of Superradiant Scattering of Laser Light from Bose-Einstein Condensates, Phys. Rev. Lett. **83**, 5202 (1999).

[6] Ö. E. Müstecaplioglu and L. You, Superradiant light scattering from trapped Bose-Einstein condensates, Phys. Rev. A **62**, 063615 (2000).

[7] H. Pu, W. Zhang, and P. Meystre, Wave Mixing of Optical Pulses and Bose-Einstein Condensates, Phys. Rev. Lett. **91**, 150407 (2003).

[8] E. D. Trifonov, On the theory of superradiant Reyleigh scattering from a Bose-Einstein condensate, JETP **93**, 969 (2001); E. D. Trifonov and N. I. Shamrov, On the theory of superradiant scattering of light from a Bose-Einstein condensate of dilute atomic gases, Opt. Spectrosc. **96**, 258 (2004).

[9] C. Benedek and M. G. Benedikt, Cooperative effects in atom field interactions in a Bose-Einstein condensate, J. Opt. B: Quantum Semiclassical Opt. **6**, S111 (2004).

[10] N. A. Vasilev, O. B. Efimov, E. D. Trifonov, and N. I. Shamrov, Semiclassical theory of coherent optical effects in Bose-Einstein condensate of dilute atomic gases, Laser Phys. **14**, 1268 (2004).

[11] L. Deng, E. W. Hagley, Q. Cao, X. Wang, X. Luo, R. Wang, M. G. Payne, F. Yang, X. Zhou, X. Chen, and M. Zhan, Observation of a Red-Blue Detuning Asymmetry in Matter-Wave Superradiance, Phys. Rev. Lett. **105**, 220404 (2010).

[12] W. Zhang and D. F. Walls, Quantum field theory of interaction of ultracold atoms with a light wave: Bragg scattering in nonlinear atom optics, Phys. Rev. A **49**, 3799 (1994).

[13] K. V. Krutitsky, F. Burgbacher, and J. Audretsch, Local-field approach to the interaction of an ultracold dense Bose gas with a light field, Phys. Rev. A **59**, 1517 (1999).

[14] O. Zobay and G. M. Nikolopoulos, Dynamics of matter-wave and optical fields in superradiant scattering from Bose-Einstein condensates, Phys. Rev. A **72**, 041604(R) (2005).

[15] O. Zobay and G. M. Nikolopoulos, Spatial effects in superradiant Rayleigh scattering from Bose-Einstein condensates, Phys. Rev. A **73**, 013620 (2006).

[16] L. Deng, M. G. Payne, and E. W. Hagley, Electromagnetic Wave Dynamics in Matter-Wave Superradiant Scattering, Phys. Rev. Lett. **104**, 050402 (2010).

[17] L. Deng, C. Zhu, and E. W. Hagley, Light-Wave Mixing and Scattering with Quantum Gases, Phys. Rev. Lett. **110**, 210401 (2013).

[18] L. Deng, C. Zhu, E. W. Hagley, and W. R. Garrett, Suppression of directional light-wave mixing in normal and quantum gases, Phys. Rev. A **88**, 043642 (2013).

[19] L. V. Hau, S. E. Harris, Z. Dutton, and C. H. Behroozi, Light speed reduction to 17 metres per second in an ultracold atomic gas, Nature (London) **397**, 594 (1999).

[20] P. W. Milonni, *Fast Light, Slow Light and Left-Handed Light* (Institute of Physics Publishing, Bristol and Philadelphia, 2005).

[21] Y. Wu and L. Deng, Ultraslow Optical Solitons in a Cold Four-State Medium, Phys. Rev. Lett. **93**, 143904 (2004).

[22] G. Huang, L. Deng, and M. G. Payne, Dynamics of ultraslow optical solitons in a cold three-state atomic system, Phys. Rev. E **72**, 016617 (2005).

[23] G. S. Agarwal and T. N. Dey, Fast light solitons in resonant media, Phys. Rev. A **75**, 043806 (2007).

[24] G. Huang, C. Hang, and L. Deng, Gain-assisted superluminal optical solitons at very low light intensity, Phys. Rev. A **77**, 011803(R) (2008).

[25] G. Dong, J. Zhu, W. Zhang, and B. A. Malomed, Polaritonic Solitons in a Bose-Einstein Condensate Trapped in a Soft Optical Lattice, Phys. Rev. Lett. **110**, 250401 (2013).

[26] M. E. Tasgin, Ö. E. Müstecaplioglu, and L. You, Creation of a vortex in a Bose-Einstein condensate by superradiant scattering, Phys. Rev. A **84**, 063628 (2011).

[27] C. Zhu, L. Deng, E. W. Hagley, and G. Huang, Optical self-focusing effect in coherent light scattering with condensates, Laser Phys. **24**, 065402 (2014).

[28] G. Huang, M. G. Velarde, and V. A. Makarov, Dark solitons and their head-on collisions in Bose-Einstein condensates, Phys. Rev. A **64**, 013617 (2001).

[29] The dimensionless beam radii of the pump and scattered fields ρ_P and ρ_S (in units of $a_\perp$) are not necessarily to be the same as the transverse size of the BEC, i.e., $a_\perp$. In the present study, we assume $\rho_P = \rho_S \equiv \rho$ with $\rho = 1$ for simplicity.

[30] A. Jeffery and T. Kawahawa, *Asymptotic Methods in Nonlinear Wave Theory* (Pitman, London, 1982).

[31] C. J. Pethick and H. Smith, *Bose-Einstein Condensation in Dilute Gases* (Cambridge University, Cambridge, England, 2008).

[32] L. P. Pitaevskii and S. Stringari, *Bose-Einstein Condensation* (Clarendon, Oxford, 2003).

[33] G. P. Agrawal, *Nonlinear Fiber Optics*, 3rd ed. (Academic, New York, 2001).